

Journal Homepage: www.journalijar.com

INTERNATIONAL JOURNAL OF ADVANCED RESEARCH (IJAR)

Article DOI:10.21474/IJAR01/22098

DOI URL: <http://dx.doi.org/10.21474/IJAR01/22098>

RESEARCH ARTICLE

LAND USE/LAND COVER DYNAMICS AND LOCAL CLIMATE CHANGE IN THE BOSSEMATIE NATURE RESERVE, COTE D'IVOIRE

Ouattara Ismaïla¹, Bogui Elie Bandama², Sawadogo Zounabo Epouse Kouyate³, Kouakou Koffi Abdelaziz⁴
and Zago Tete Morel¹

1. Department of Mines and Reservoirs, Faculty of Geological and Mining Sciences, University of Man, BP 20 Man, Cote d'Ivoire.
2. Unit of Training and Research in Engineering, Agronomy, Forestry and Environmental Sciences, University of Man, BP 20 Man, Cote d'Ivoire.
3. Agropastoral Management Institute, Peleforo Gon Coulibaly University, BP 1328 Korhogo, Cote d'Ivoire.
4. Department of Geoscience, Peleforo Gon Coulibaly University, BP 1328 Korhogo, Cote d'Ivoire.

Manuscript Info

Manuscript History

Received: 04 September 2025

Final Accepted: 06 October 2025

Published: November 2025

Key words:-

Deforestation, climate variability,
microclimate, Temperature, Rainfall,
Bossématié Nature Reserve.

Abstract

The study on the impact of land use and land cover (LULC) on climate has highlighted the close interactions between spatial dynamics of terrestrial cover and climatic variables within the Bossématié Nature Reserve (BNR) in Côte d'Ivoire. A diachronic analysis of land use and land cover changes over the 1990–2020 period reveals a significant decline in dense vegetation, replaced by agricultural land, human settlements, and degraded surfaces. This dynamic is primarily driven by the intensification of anthropogenic activities in and around the reserve. However, climate evolution, particularly through the analysis of temperature and precipitation time series, indicates a trend shift. A progressive rise in temperatures has been observed since 1986, along with an increase in annual rainfall totals after 2008. These changes coincide with disturbances in vegetation cover, suggesting a probable link between deforestation, alteration of the local microclimate, and redistribution of rainfall regimes. These findings underscore the need for improved land management practices around protected areas to mitigate adverse effects on ecosystems and local climate. It is therefore essential to integrate climate considerations into spatial planning policies and to strengthen biodiversity conservation efforts within the Bossématié Nature Reserve.

"© 2025 by the Author(s). Published by IJAR under CC BY 4.0. Unrestricted use allowed with credit to the author."

Introduction:-

The relationship between land use and climate constitutes one of the major challenges of contemporary environmental research. Indeed, land-use changes directly influence local, regional, and global climates (IPCC, 2019). Human activities have profoundly altered the Earth's surface, producing multiple effects on climatic regimes. According to Foley et al. (2005), more than 40% of the terrestrial surface is currently exploited for agricultural or urban purposes,

Corresponding Author:- Ouattara Ismaïla

Address:- Department of Mines and Reservoirs, Faculty of Geological and Mining Sciences, University of Man, BP 20 Man, Cote d'Ivoire.

thereby altering the planet's energy and water balances. Deforestation, urbanization, agricultural intensification, and land artificialization modify heat fluxes, greenhouse gas emissions, and biogeochemical cycles (Turner et al., 2007). Moreover, the reduction of forested areas contributes to the loss of carbon sinks, thereby amplifying the greenhouse effect (Bonan, 2008). According to Pielke et al. (2002), the effects of land-use and land-cover changes can be comparable to those of increased atmospheric CO₂ concentrations in certain regional contexts. Conversely, climate itself influences land use patterns. Changes in rainfall regimes and temperature affect agricultural potential and urban dynamics (Lambin & Geist, 2006). Thus, climate evolution requires adjustments in land management, particularly concerning agricultural adaptation (Verburg et al., 2011). As emphasized by Li et al. (2017), the feedbacks between climate and land use call for a systemic and forward-looking approach to ensure sustainable spatial planning. According to FAO (2020), sustainable land use management can play a key role in mitigating climate change. Consequently, integrating climate considerations into land-use planning has become an imperative for sustainable development policies (UNEP, 2016). At the local scale, as Bonan (2008) points out, forest loss can lead to regional warming and reduced rainfall. In the Ivorian context, N'Dri et al. (2018) show that forest reserves are under increasing pressure, which weakens their function as carbon sinks. Therefore, this study adopts an integrated geographical and climatic approach to explore the effects of spatial land-use evolution on the microclimate of the Bossématié Nature Reserve (BNR).

Materials and Methods :-

Location of the Bossématié Nature Reserve (BNR) :

Located in the Abengourou region, in the southeastern part of Côte d'Ivoire, the Bossématié Nature Reserve (BNR) and its surrounding area are the focus of this study. It lies between longitudes 03°38'00" and 03°27'00" West and latitudes 06°20'30" and 06°31'30" North (Figure 1). The Department of Abengourou is part of the Moyen-Comoé administrative region, of which it serves as the regional capital. It covers an area of 5,043 km², representing approximately 75% of the regional territory and 2% of the national territory. The department is bounded to the north by the Departments of Agnibilékro and Daoukro, to the south by Alépé and Aboisso, to the east by the Republic of Ghana, and to the west by Bongouanou and Adzopé (Figure 1). The sub-equatorial climate of the region is characterized by four distinct seasons: the major rainy season (mid-March to mid-July), the short dry season (mid-July to August), the minor rainy season (September to mid-November), and the long dry season (mid-November to mid-March) (ANADER, 2020). The hydrographic network is dominated by the Comoé River, along with its main tributaries, the Béki and Manzan rivers (Figure 1). The economic activities of the Department are primarily based on the primary sector, with agriculture representing more than 90% of the total local economy. The main cash and food crops include coffee, cocoa, rubber (Hevea), and market garden products, which serve as the key drivers of the Department's economy. The agricultural population is composed of autochthonous groups, internal migrants, and allochthonous settlers (ANADER, 2020).

Satellite and cartographic data :

The Landsat satellite image bands (B1, B2, B3, and B4) were used to map land use/land cover (LULC) dynamics. Table 1 provides details of the different images. These images are freely available and can be downloaded from the USGS website (<https://earthexplorer.usgs.gov/>). For the purpose of a diachronic study of LULC dynamics and considering the availability of satellite images, images from 1990, 2000, 2010, and 2020 were selected.

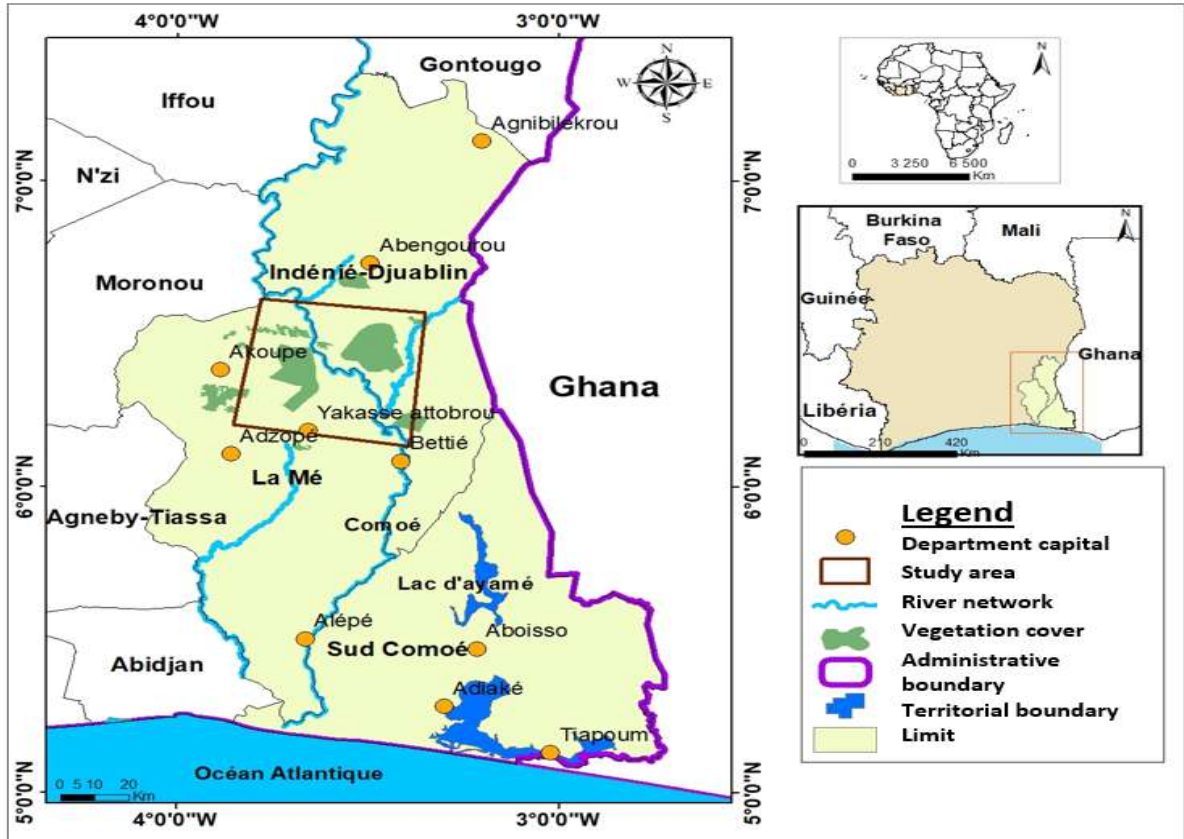


Figure 1: Location of the Bossématié Nature Reserve (BNR)

Table 1: List of Landsat satellite images used for diachronic analysis

Image Type	Date
Landsat 5 TM	31 December 1990
Landsat 5 TM	03 January 2000
Landsat 7 ETM+	04 February 2010
Landsat 8 OLI	04 ebruary 2020

Climatic Data :

For this study, only monthly and annual precipitation and temperature data from the Abengourou station (latitude 6.7167, longitude -3.4833) were used. Satellite-derived data were preferred over ground-based observations. This choice is justified by the fact that the temperature measurements for this station are recorded at the Dimbokro synoptic station, an area considered the hottest in Côte d'Ivoire. Using these temperature data togetherwith precipitation data from Abengourou wouldintroducebias into the analysis. Therefore, the POWER Data Access product (POWER | Data Access Viewer (nasa.gov)) was selected, as it provides all relevant climatic variables for a single location and is widelyrecognized for its reliability. The POWER Data Access database includesgeospatial parameters related to meteorology and solarenergy. Solar data in POWER are derived from satellite observations, from which surface insolation values are calculated. Meteorological parameters are based on the MERRA-2 assimilation model, and uncertaintyestimates are derived fromcomparisonswithground-based measurements.

Land use/land cover characterizationtechnique:

In this study, the mapping of land use/land cover (LULC) units was performed using the Semi-Automatic Classification Plugin (SCP) for QGIS, developed and maintained by Congedo (2021). This comprehensivetoolallows both supervised and unsupervised classification of satellite images, as well as their download, pre-processing, and post-processing. The method used to map LULC unitsconsisted of three main steps: pre-processing, processing, and post-processing. Landsat images from 1990, 2000, 2010, and 2020, obtained from the USGS (United States Geological Survey) website, were used to detect land-use changes in the BossématiéClassified Forest. The

supervised classification was based on the selection of five LULC classes: water, built-up areas, vegetation, crops, and bare soil (Table 2).

Table 2: Description of Land Use/Land Cover classes

Class	Description
Water	Rivers, lakes, reservoirs
Built-up	Urban areas, rural settlements, dams
Vegetation	Plant formations dominated by scattered trees and grasses
Crops	Food crops, sparsely vegetated cover, fallow land, degraded forest
Bare Soil	Areas with no vegetation cover

Accuracy assessment of thematic maps :

It is important to note that the quality of thematic maps derived from remote sensing data can be evaluated and expressed quantitatively. A classification error therefore represents a discrepancy between the thematic map and the actual ground situation (as determined through field surveys). Conventional methods for assessing the thematic accuracy of a map include the error matrix and the Kappa coefficient (N'Da et al., 2008). The Kappa coefficient measures the agreement between the classified results and ground truth within the confusion matrix. It ranges from 0 to 1 and is divided into five categories, where values closer to 1 indicate an almost perfect agreement (Caloz et al., 1993). The Kappa coefficient is calculated using the following formula:

$$K = \frac{N \sum_{i=1}^r x_{ii} - \sum_{i=1}^r (x_{i+} \cdot x_{i-})}{N^2 - \sum_{i=1}^r (x_{i+} \cdot x_{i-})} \quad (1)$$

Where:

- r is the number of rows in the confusion matrix,
- x_{ii} is the number of observations in row i and column i (diagonal),
- x_{i+} is the total number of observations in row i ,
- x_{i-} is the total number of observations in column i ,
- N is the total number of observations in the matrix.

Characterization of climate variability :

Pettitt's change-point Test :

The non-parametric Pettitt test is used to detect changes in the central tendency of a time series (Pettitt, 1979). The null hypothesis (H_0) assumes no change, while the alternative hypothesis (H_1) assumes a change. This test was applied to the annual precipitation series from the Abengourou station (1981–2022) to identify any significant shifts in the mean over time. In this method, the test is implemented as described by Verstraeten et al. (2006), where the ranks r_1, \dots, r_n of the observations X_1, \dots, X_n are used to compute the test statistic:

$$U_k = 2 \sum_{i=1}^k r_i - k(n + 1) \quad k = 1, \dots, n \quad (2)$$

The test statistic is defined as the maximum of the absolute values of the vector:

$$\hat{U} = \max |U_k|$$

The probable change point K is located where \hat{U} reaches its maximum. The approximate probability for a two-sided test is calculated using Equation 3:

$$p = 2 \exp^{-6K^2 / (T^3 + T^2)} \quad (3)$$

The Pettitt test was implemented using the Trend package (Pohlert, 2015) from the CRAN repository in R.

Ombrothermic curve :

An ombrothermic diagram is a specific type of climatic chart that represents the monthly variations of temperature and precipitation over a year using standardized scales: one graduation on the precipitation scale corresponds to two graduations on the temperature scale ($P = 2T$) (Charre, 2007). This diagram highlights dry periods (shown in yellow), which are defined by the precipitation curve (here represented as a blue histogram) falling below the temperature curve (here represented as a red line).

Results:-

Diachronic Analysis of Land Use/Land Cover in and around the RNB :-

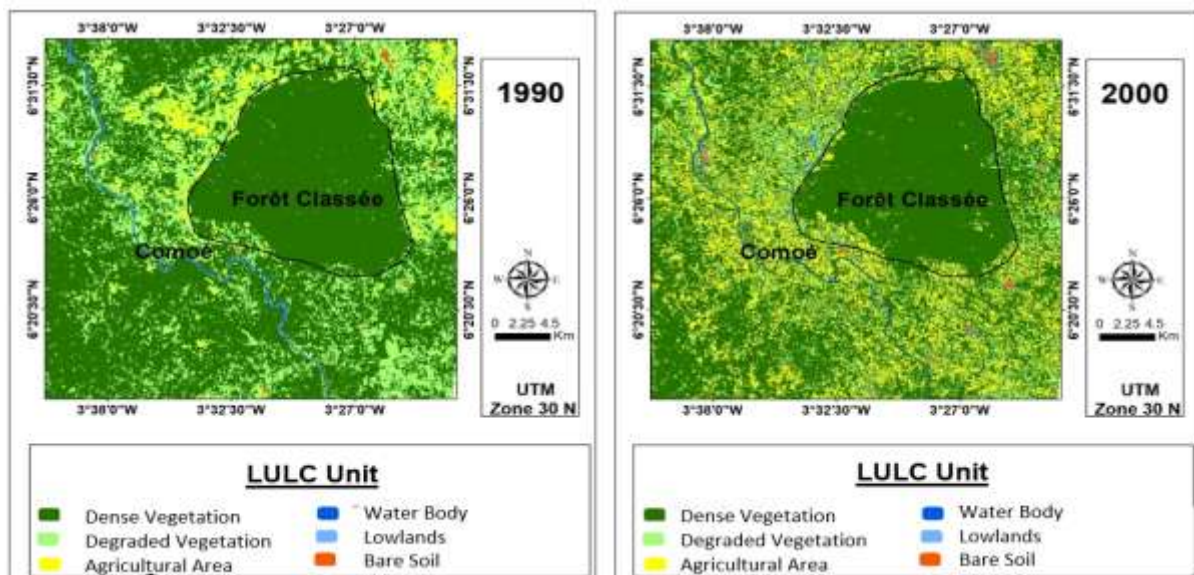
The land use/land cover (LULC) maps for 1990, 2000, 2010, and 2020, derived from the interpretation of Landsat images, allowed the characterization of vegetation cover changes and anthropogenic activities in and around the Bossématié Natural Reserve (RNB). For this study, six LULC classes were defined: dense vegetation, degraded vegetation, water bodies, lowlands, agricultural areas, and settlements with bare soil. The overall accuracy ranged from 71% to 80%, and the Kappa coefficient ranged from 0.66 to 0.74 across all four LULC maps, reflecting the reliability of the classification. Figures 2 and 3 illustrate the evolution of vegetation cover and the expansion of anthropogenic activities from 1990 to 2020 in and around the RNB. In 1990, the area was dominated by dense vegetation. Agricultural areas were sparse, mostly located in the northeast and north-central peripheries. The classified forest was predominantly covered by dense vegetation, with degraded vegetation appearing only in certain locations within the study area. Settlements and bare soil were almost absent, except for small patches representing village sites.

By 2000, there was an increase in agricultural lands and a significant degradation of vegetation cover throughout the zone, leading to continued soil exposure. Within the RNB, dense vegetation remained dominant, but the peripheries began to experience encroachment from anthropogenic activities. In 2010 and 2020, the area experienced a significant expansion of agricultural lands and settlements, spreading from the southeast and central parts toward the north, accompanied by degraded forest covering nearly the entire site. The vegetation cover in this zone is at risk, and the water courses remain potentially vulnerable due to ongoing agricultural activities. The diagrams below (Figure 3) show the spatial evolution (in terms of percentage) of land use/land cover classes. Dense forest, which covered 925.85 km² (70.49%) in 1990, gradually decreased to 398.85 km² (20.59%) in 2020. A proliferation of settlements and agricultural areas has been observed over these years. Settlements, which occupied 1.87 km² (0.14%) in 1990, increased to 27.46 km² (2.07%) in 2020, while agricultural lands expanded from 58.1 km² (4.42%) in 1990 to 372.012 km² (28.16%) in 2020. The variation in the area occupied by water bodies was not significant between 1990 and 2020.

Variability of climatic parameters at the Abengourou rainfall station:

Annual variability :

Based on the Pettitt test, a break in stationarity of the annual mean temperature and annual rainfall series is observed at a significance level of $\alpha = 0.05$. This break occurs in 1986 for the temperature time series, while for the rainfall series it occurs in 2008 (Table 3). These breaks indicate a temperature increase after 1986 and a rainfall increase after 2008 (Figures 4 and 5). Boxplots clearly show that annual mean temperatures were around 25.5 °C between 1981 and 1986, increasing by approximately 1 °C over the period 1987–2022 (Figure 4). Annual rainfall, with an increase of about 200 mm, also rises after the break, with a median value of 1600 mm (Figure 5).



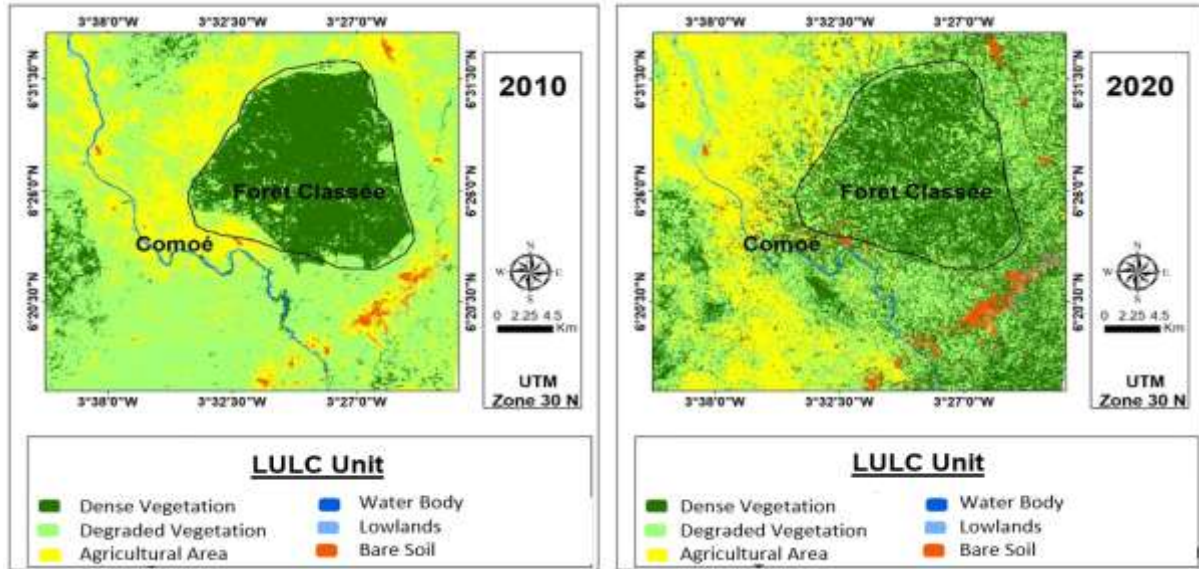


Figure 2:Decadal evolution (1990, 2000, 2010, and 2020) of Land Use/Landin and around the RNB

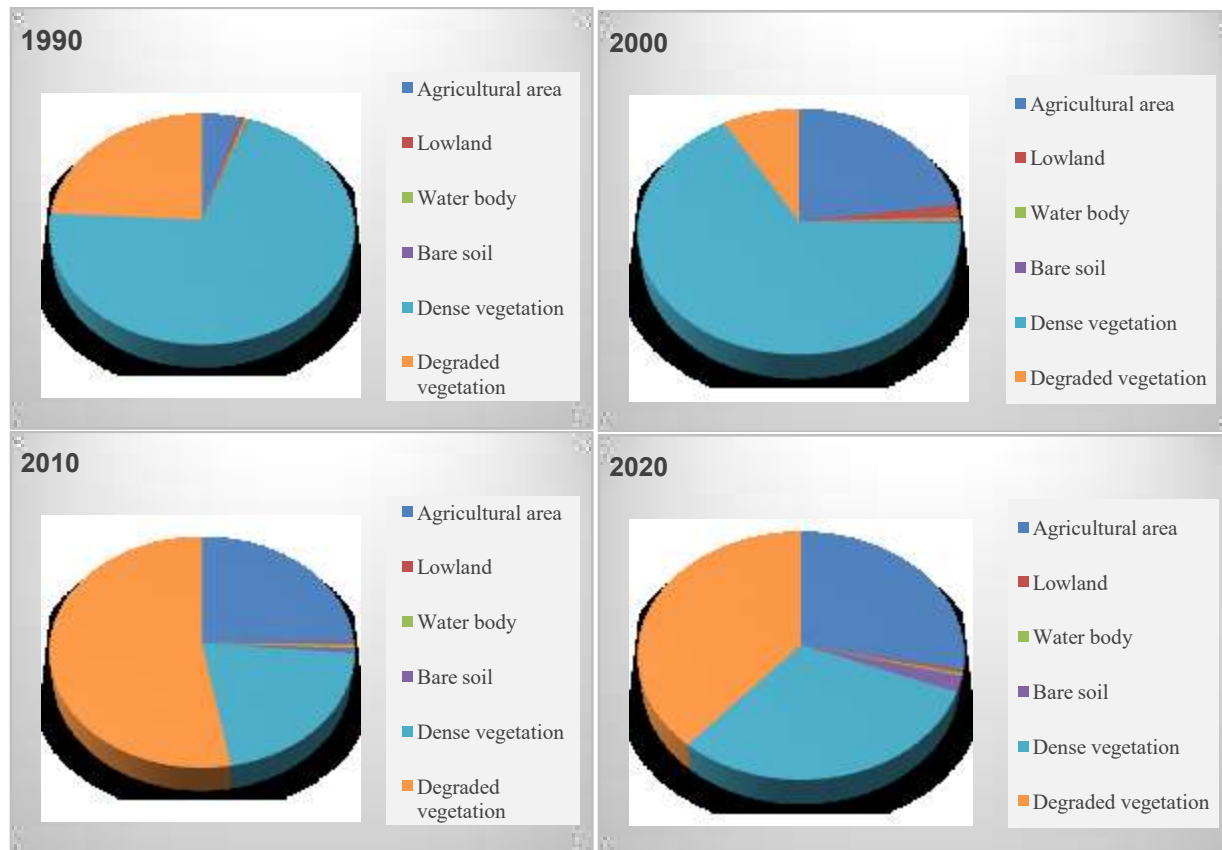


Figure 3: Percentage distribution of Land Use/Land Cover classes in the RNB in 1990, 2000, 2010, and 2020

Table 3:Pettitt test for breaks in annualmean temperature and annualrainfall series

Parameter	Pettitt Test at $\alpha = 0.05$		
	U*	p-value	Break year
Annual Temperature	151	0.3294	1986
Annual Rainfall	180	0.1542	2008

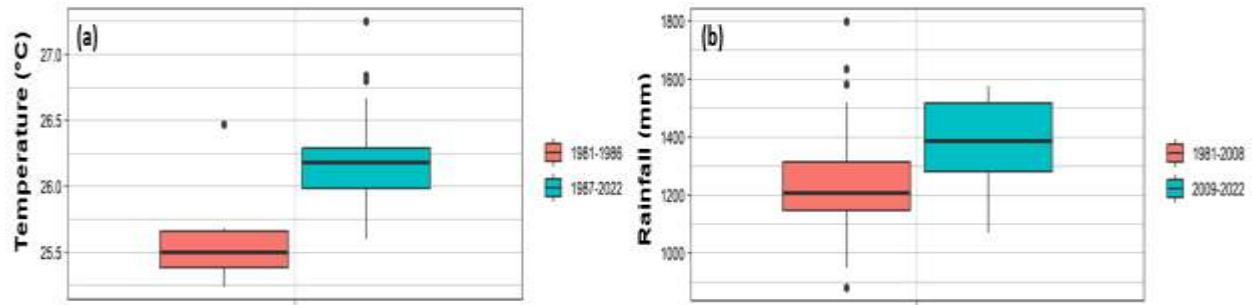


Figure 4: Statistical distribution of annual mean after and before the break respectively for temperature (a) and rainfall (b)

Monthly variability :

The sub-equatorial type of climate in the RNB environment, characterised by four (4) seasons (two dry seasons and two rainy seasons), is better reflected in the distribution of monthly rainfall totals than in that of temperatures (Figures 6 and 7). With regard to temperature, the months from November to May are the warm months over the study period, with temperatures ranging between 27 °C and 31 °C. The hottest months are January, February, and March, with average temperatures around 30 ± 1 °C (Figure 6).

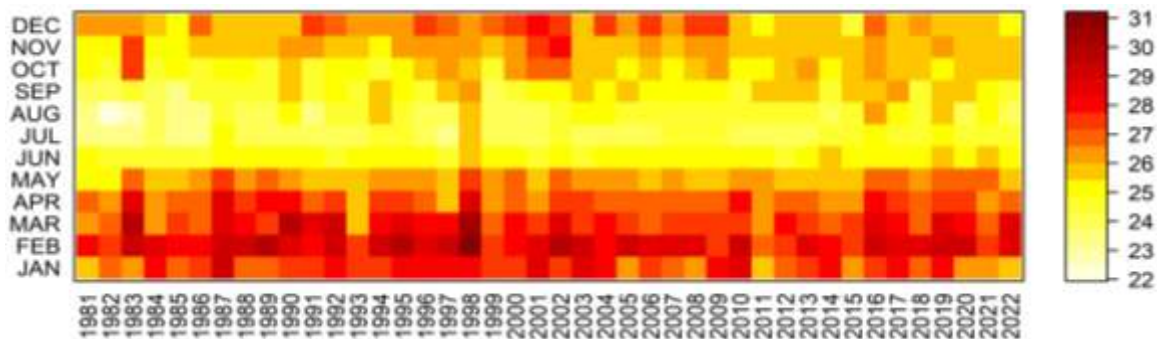


Figure 6: Interannual variability of monthly mean temperatures at the Abengourou station

An alternation of two wet seasons is observed in Figure 7. The larger, more marked wet season, with average monthly rainfall heights ranging from 200 mm to 400 mm, extends from April to July. Following the rainfall disruption of 2008, characterized by an increase in annual totals, there is a shortening of this season by one month. It now spans from April to June. The shorter wet season begins in September and ends in October, with rainfall depths between 100 mm and 200 mm. Consequently, the months comprising the wet season have decreased. Nevertheless, the annual rainfall totals have increased. This would be explained by a redistribution of rainfall from July to other months that became wetter after 2008. Indeed, this pattern is observed for the months of May and June. The dry short season runs from July to August, while the long dry season extends from November to March. The monthly rainfall totals during the dry season are less than 50 mm.

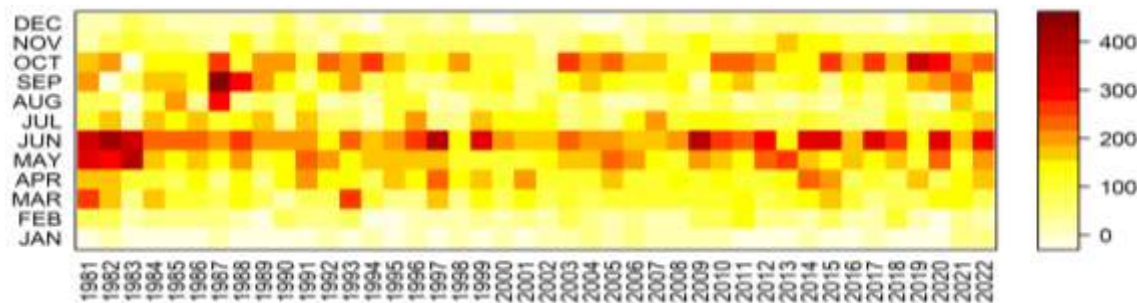
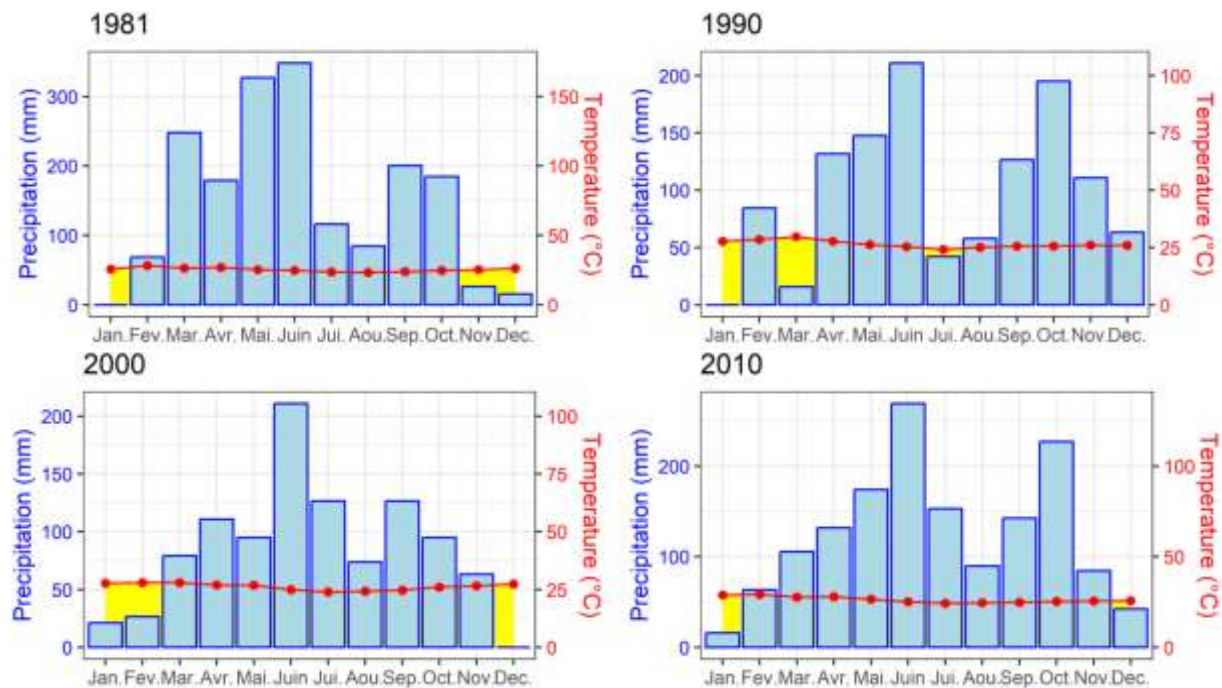


Figure 7: Interannual variability of monthly rainfall totals at Abengourou station

Variability of the climatic seasons at Abengourou station :

The years chosen to establish the land-cover maps are the same as those used for the rainfall–temperature curves (with the exception of the 1981 curve). The aim is to assess the link between vegetation and climate. In 1990, the periphery and even the core of the Reserved Natural Biodiversity (RNB) still retained vegetation integrity. The area is dominated by very dense vegetation. Climatically, only two seasons were distinguishable. The dry season was shorter, lasting three months (November, December, and January). In contrast, the wetter season was longer, spanning nine months from February to October, though February could be considered part of the dry season given its low rainfall. Additionally, July and August could be regarded as part of a small dry season since their monthly totals are among the lowest, except February; however, based on the interpretation of the rainfall–temperature curve, these months are regarded as wet in 1990. By 2000, there is an observed expansion of agricultural land and substantial degradation of vegetation cover across the study area. There is stronger anthropogenic pressure from the periphery of the RNB. The analysis of the 2000 curve indicates that August and December are at the margin of the wet category. Four seasons are observed: a large dry season from December to March (with February being unusually wet), a first wet season from April to June, a shorter second dry season (July and August), and finally a second dry season from September to November.

In 2010 and 2020, there is strong expansion of agricultural land and habitats, with widespread degraded forest across nearly the entire area (including the RNB). However, the rainfall–temperature curves for 2010 and 2020 show a long wet season (March to November). Only December, January, and February remain dry. This pronounced, multi-month wet character (which was originally a dry period) in a context of substantial vegetation loss could be explained by a rebound in rainfall. Indeed, after the 2008 disruption, there was an increase in annual totals. Concurrently, the wet months experienced a reduction in their monthly totals. From 1990, these totals ranged between 100 mm and 300 mm. From 2000 to 2010, monthly totals ranged from 75 mm to 2000 mm. The direct consequence is a rise in the dry-month totals that resemble wet months. A similar dynamic is observed in 2020, notwithstanding the advanced degradation of the vegetation cover both within and outside the RNB. An increase in rainfall during the wet months, fluctuating between 100 mm and 300 mm, is observed.



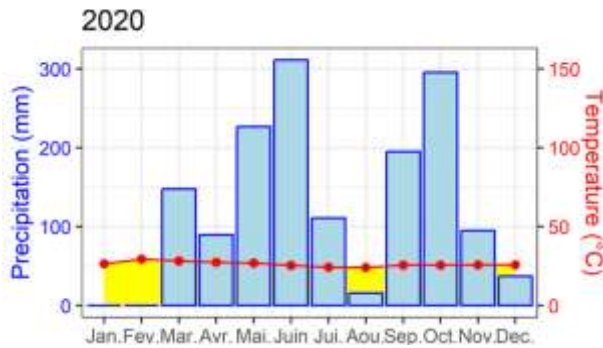


Figure 8: Rainfall–temperature curve at Abengourou station for the years 1990, 2000, 2010, and 2020

Discussion:-

The diachronic analysis of land cover in and around the Bossématié National Reserve (RNB) between 1990 and 2020 highlights a spatio-temporal dynamic marked by a progressive regression of dense vegetation in favour of anthropogenic activities, primarily agriculture. This trend confirms observations from numerous earlier studies that link land cover changes to increased pressure on forest ecosystems (FAO, 2016; IPCC, 2021). Between 1990 and 2000, the substantial expansion of agricultural areas observed at the expense of natural vegetation formations suggests an intensification of natural resource exploitation linked to demographic growth and the expansion of cultivable land. The conversion of forested spaces into agricultural or residential zones inevitably leads to biomass loss, thereby reducing carbon sequestration capacity (Achard et al., 2014). This loss of vegetation also impacts the local microclimate, reducing air humidity and increasing surface temperatures (Lambin & Geist, 2006). Data show that by 2000, the periphery of the RNB already exhibited notable degradation, reflecting a weakening of the reserve's ecological functions. This trend continued to 2020, with heightened human activities in the immediate vicinity of the reserve. This phenomenon, identified as the edge effect, intensifies habitat fragmentation and exposes central areas to ecological changes (Hansen et al., 2013). The climatic impact of these changes is twofold: first, the reduction of dense vegetation decreases albedo, favouring heat accumulation at the surface (Bonan, 2008); second, it disrupts hydrological fluxes by altering evapotranspiration cycles, which may modify local rainfall (De Noblet-Ducoudré et al., 2012). The recurrence of these perturbations over time can contribute to a trend of localised climate warming in the region.

The reliability of the classifications (Kappa between 0.66 and 0.74) strengthens the validity of the results. Nevertheless, uncertainties persist, notably related to Landsat image resolution and potential misclassification between degraded vegetation and bare soil. Future research would benefit from integrating local climatic data (temperatures, rainfall) and field observations to refine links between land-cover dynamics and observed climatic variations. In 2010 and 2020, the deforestation trend intensified within and around the RNB. The retreat of dense forest cover in favour of agricultural land and habitats indicates an acceleration of anthropogenic dynamics already begun in previous decades. This landscape transformation is particularly pronounced in the south-east and centre-north of the site, where there is a growing concentration of human activities. The decline in dense forest area, from 925.85 km² (70.49%) in 1990 to 398.85 km² (20.59%) in 2020, is alarming. This nearly 57% retreat over thirty years signals ongoing pressure on forest resources. In parallel, agricultural area was multiplied by more than six, from 58.1 km² (4.42%) to 372.012 km² (28.16%). This massive expansion of cultivated land is symptomatic of intensified agricultural practices, often extensive and unsustainable.

Human habitats also grew significantly, from 1.87 km² (0.14%) to 27.46 km² (2.07%) between 1990 and 2020. This progressive urbanisation, though relatively modest in proportion, acts as a catalyst for habitat fragmentation, reducing ecological continuity of the RNB. The apparent stability of water courses should not mask their increasing vulnerability to soil erosion, siltation, and agricultural pollution. The reduction of vegetation, which normally protects soils, worsens runoff and jeopardises water resources, particularly during periods of heavy rainfall. These transformations markedly impact the local climate, chiefly through reduced evapotranspiration, increased surface temperatures, and altered rainfall regimes. The works of Foley et al. (2005) and DeFries et al. (2010) have demonstrated that such land-use transitions influence climatic processes at the regional scale. The analysis of climate time series using Pettitt's non-parametric test revealed significant breaks at the $\alpha = 0.05$ threshold in trends of annual mean temperatures and annual rainfall totals. These breaks indicate a notable change in the local climate regime. The stationarity break observed in 1986 in the mean annual temperature series marks the onset of a

warmer period. Indeed, temperatures, which fluctuated around 25.5 °C before 1986, show an increase of about 1 °C in the post-1986 period (1987–2022). This rise, though apparent at the local scale, aligns with the global warming trend, as supported by IPCC (2021) and Nicholson (2014) in West Africa. Regarding rainfall, the break detected in 2008 indicates a shift in the rainfall regime. The series shows an increase in precipitation, with an uptick of around 200 mm relative to the preceding period and a median height reaching 1600 mm after the break. This gradual return to higher rainfall levels could be related to natural variability (Atlantic multidecadal oscillation) or to changes in atmospheric circulation regimes. Box-and-whisker plots (Figures 4 and 5) clearly illustrate these breaks: dispersion of values is greater after the breaks, indicating increased climate variability post-1986 for temperature and post-2008 for rainfall. These climatic changes can have a direct impact on ecosystems and land use, particularly in forest transition zones such as the RNB. Temperature increases could intensify evapotranspiration and weaken vegetation cover, while increased rainfall, if poorly distributed, could exacerbate erosion or favour more extensive cropping, further aggravating deforestation.

The synchronized analysis of land-cover maps and rainfall–temperature curves helps to better delineate the potential influence of climate on vegetation dynamics, but also the growing impact of human activities. In 1990, dense vegetation predominated in both the core and the periphery of the Bossématié National Reserve (RNB). This situation is consistent with the relatively humid climatic conditions of that year. Indeed, the wet season extended for nearly nine months, with July and August only mildly deficient, yet still classified as wet according to the rainfall–temperature curves. Such moisture favours plant growth and the maintenance of forest ecosystems. However, by 2000, substantial degradation of vegetation is observed, with a significant increase in agricultural lands and greater anthropogenic pressure at the periphery of the reserve. This degradation is reinforced by the emergence of four climatic seasons, indicating fragmentation of the rainfall regime. A longer dry season and a double wet season, interspersed with dry periods (July–August), are observed, which could affect natural regeneration of vegetation. Taken together, these factors indicate that while climate clearly plays a role in structuring ecosystems, the most marked changes between 1990 and 2000 appear more linked to agricultural expansion and resource exploitation, signs of increasing anthropogenic pressure.

Thus, the reduced humidity combined with unsustainable practices exacerbates the vulnerability of the classified forest. The 2010s and 2020s mark a critical stage in the land-cover dynamics around and within the RNB. The maps reveal a strong regression of vegetation cover, now dominated by degraded forest, agricultural land, and habitation zones, signs of advanced anthropisation of the area. Paradoxically, climate conditions, according to the rainfall–temperature curves, show an extension of the wet season from March to November, compared with only nine months in 1990. This phenomenon is consistent with Pettitt test results, which indicate a significant increase in rainfall totals after 2008. However, this relative improvement in climate does not translate into vegetation recovery. On the contrary, vegetation loss intensifies despite the increase in annual rainfall, underscoring the predominance of anthropogenic factors over landscape dynamics. Indeed, increases in rainfall during historically dry months (December to February) do not compensate for rising agricultural pressure, deforestation, and urban expansion. In other words, the ecological resilience of the RNB appears surpassed by human transformations, even in a climate appearing more favourable. This disconnect between climatic conditions and the state of the vegetation cover reflects an imbalance where anthropogenic effects now outweigh natural regulations, compromising the ecological sustainability of the reserve.

Conclusion:-

The study on the impact of land use on the climate, with the Bossématié National Reserve (RNB) as its setting, has highlighted the close interactions between spatial dynamics of the terrestrial cover and climatic variables. The diachronic analysis of land use over the period 1990–2020 reveals a marked regression of dense vegetation in favour of agricultural lands, habitats, and degraded surfaces. This dynamic results primarily from the intensification of anthropogenic activities around and within the reserve. Concurrently, climatic evolution, notably through time series of temperature and rainfall, shows a shift in trend. A progressive rise in temperatures is observed from 1986, together with an increase in annual rainfall totals after 2008. These changes coincide with perturbations to the vegetation cover, suggesting a probable link between deforestation, modification of the local microclimate, and the redistribution of rainfall regimes. These findings underscore the need for improved land-use management around protected zones to limit adverse effects on ecosystems and on local climate. It is therefore crucial to integrate climate considerations into land-use planning policies and to strengthen biodiversity conservation actions within the RNB.

References:-

1. Nicholson, S. E. (2014). A detailed look at the recent drought situation in the Greater Horn of Africa. *Journal of Arid Environments*, 103, 71–79. <https://doi.org/10.1016/j.jaridenv.2013.12.003>.
2. Intergovernmental Panel on Climate Change (IPCC). (2021). *Climate Change 2021: The Physical Science Basis. Contribution of Working Group I to the Sixth Assessment Report of the Intergovernmental Panel on Climate Change*. Cambridge University Press. <https://doi.org/10.1017/9781009157896>
3. Foley, J. A., DeFries, R., Asner, G. P., Barford, C., Bonan, G., Carpenter, S. R., ... & Snyder, P. K. (2005). Global consequences of land use. *Science*, 309(5734), 570–574. <https://doi.org/10.1126/science.1111772>
4. DeFries, R. S., Rudel, T., Uriarte, M., & Hansen, M. (2010). Deforestation driven by urban population growth and agricultural trade in the twenty-first century. *Nature Geoscience*, 3(3), 178–181. <https://doi.org/10.1038/ngeo756>
5. Achard, F., Beuchle, R., Mayaux, P., Stibig, H.-J., Bodart, C., Brink, A., ... & Simonetti, D. (2014). Determination of tropical deforestation rates and related carbon losses from 1990 to 2010. *Global Change Biology*, 20(8), 2540–2554. <https://doi.org/10.1111/gcb.12676>
6. Hansen, M. C., Potapov, P. V., Moore, R., Hancher, M., Turubanova, S. A., Tyukavina, A., ... & Townshend, J. R. G. (2013). High-resolution global maps of 21st-century forest cover change. *Science*, 342(6160), 850–853. <https://doi.org/10.1126/science.1244693>
7. Bonan, G. B. (2008). Forests and climate change: Forcings, feedbacks, and the climate benefits of forests. *Science*, 320(5882), 1444–1449. <https://doi.org/10.1126/science.1155121>
8. FAO. (2016). *État des forêts du monde 2016. Les forêts et l’agriculture : défis et opportunités en lien avec l’utilisation des terres*. Organisation des Nations Unies pour l’alimentation et l’agriculture.
9. IPCC. (2021). *Climate Change 2021: The Physical Science Basis. Contribution of Working Group I to the Sixth Assessment Report of the Intergovernmental Panel on Climate Change*. Cambridge University Press.
10. Intergovernmental Panel on Climate Change. (2019). *Climate Change and Land: An IPCC Special Report on Climate Change, Desertification, Land Degradation, Sustainable Land Management, Food Security, and Greenhouse Gas Fluxes in Terrestrial Ecosystems*.
11. Foley, J. A., DeFries, R., Asner, G. P. (2005). Global consequences of land use. *Science*, 309(5734), 570–574.
12. Turner, B. L., Lambin, E. F., & Reenberg, A. (2007). The emergence of land change science for global environmental change and sustainability. *Proceedings of the National Academy of Sciences*, 104(52), 20666–20671.
13. Pielke, R. A., Marland, G., Betts, R. A., Chase, T. N., Eastman, J. L., Niles, J. O., ... & Running, S. W. (2002). The influence of land-use change and landscape dynamics on the climate system: relevance to climate-change policy beyond the radiative effect of greenhouse gases. *Philosophical Transactions of the Royal Society A: Mathematical, Physical and Engineering Sciences*, 360(1797), 1705–1719.
14. Verburg, P. H., Neumann, K., & Nol, L. (2011). Challenges in using land use and land cover data for global change studies. *Global Change Biology*, 17(2), 974–989.
15. Li, Y., Fu, H., Yu, X., & Guo, L. (2017). Impacts of land use change on regional climate: A review. *Advances in Meteorology*, 2017, Article ID 3250385.
16. FAO. (2020). *The State of the World’s Forests 2020. Forests, biodiversity and people*. Food and Agriculture Organization of the United Nations.
17. United Nations Environment Programme. (2016). *Global Environment Outlook GEO-6: Regional Assessments*. Nairobi, Kenya.
18. N’Dri, J. K., Koné, N. A., Koffi, K. J. P., et al. (2018). Analyse de l’occupation du sol et dynamique spatio-temporelle du couvert végétal de la Réserve de Bossématié (Est de la Côte d’Ivoire). *Journal of Applied Biosciences*, 126, 12664–12676.